doi:10.1016/j.jmb.2003.12.031 J. Mol. Biol. (2004) 336, 395–408

JMB

Available online at www.sciencedirect.com

SCIENCE DIRECT®

ELSEVIER

DNA-binding Orientation and Domain Conformation of the *E. coli* Rep Helicase Monomer Bound to a Partial Duplex Junction: Single-molecule Studies of Fluorescently Labeled Enzymes

Ivan Rasnik[1]†, Sua Myong[1]†, Wei Cheng[2], Timothy M. Lohman[2] and Taekjip Ha[1]*

[1]*Department of Physics University of Illinois at Urbana-Champaign, Urbana IL 61801, USA*

[2]*Department of Biochemistry and Molecular Biophysics Washington University School of Medicine, St. Louis, MO 63110, USA*

**Corresponding author*

The SF1 DNA helicases are multi-domain proteins that can unwind duplex DNA in reactions that are coupled to ATP binding and hydrolysis. Crystal structures of two such helicases, *Escherichia coli* Rep and *Bacillus stearothermophilus* PcrA, show that the 2B sub-domain of these proteins can be found in dramatically different orientations (closed *versus* open) with respect to the remainder of the protein, suggesting that the 2B domain is highly flexible. By systematically using fluorescence resonance energy transfer at the single-molecule level, we have determined both the orientation of an *E. coli* Rep monomer bound to a 3′-single-stranded-double-stranded (ss/ds) DNA junction in solution, as well as the relative orientation of its 2B sub-domain. To accomplish this, we developed a highly efficient procedure for site-specific fluorescence labeling of Rep and a bio-friendly immobilization scheme, which preserves its activities. Both ensemble and single-molecule experiments were carried out, although the single-molecule experiments proved to be essential here in providing quantitative distance information that could not be obtained by steady-state ensemble measurements. Using distance-constrained triangulation procedures we demonstrate that in solution the 2B sub-domain of a Rep monomer is primarily in the "closed" conformation when bound to a 3′-ss/ds DNA, similar to the orientation observed in the complex of PcrA bound to a 3′-ss/ds DNA. Previous biochemical studies have shown that a Rep monomer bound to such a 3′-ss/ds DNA substrate is unable to unwind the DNA and that a Rep oligomer is required for helicase activity. Therefore, the closed form of Rep bound to a partial duplex DNA appears to be an inhibited form of the enzyme.

Keywords: helicase; protein conformation; single molecule spectroscopy; fluorescence resonance energy transfer

Introduction

Helicases unwind double-stranded (ds) nucleic acids to generate the single-stranded (ss) intermediates that are essential for many cellular processes.[3] These enzymes also translocate along nucleic acids using the chemical energy from the binding and/or hydrolysis of ATP or other nucleoside triphosphates and hence are motor proteins. As such, a helicase must couple its conformational changes resulting from ATP binding and hydrolysis to DNA unwinding and translocation. Ideally, in order to probe the mechanisms of these enzymes, one would like to measure real-time structural changes of a helicase–DNA complex during each reaction step. Single-molecule fluorescence techniques[4,5] are promising for this goal because they can detect the conformational changes of individual bio-molecules with

† I.R. & S.M. contributed equally to this work.

Abbreviations used: ss, single-stranded; ds, double-stranded; FRET, fluorescence resonance energy transfer; PEG, poly-ethylene glycol.

E-mail address of the corresponding author: tjha@uiuc.edu

millisecond time resolution under physiological conditions.

Previously, we combined the single-molecule fluorescence approach and a surface immobilization scheme which does not interfere with biological activity to probe the DNA unwinding mechanism of *Escherichia coli* Rep helicase.[2] Fluorescence resonance energy transfer (FRET) between fluorophores attached to the DNA reported the structural changes induced by the action of the enzyme, allowing us to measure DNA unwinding of only a few base-pairs and to detect unwinding stalls, DNA rewinding, and re-initiation of unwinding by a stalled enzyme–DNA complex, and to deduce their underlying mechanisms.[2]

Rep, *E. coli* UvrD and *Bacillus stearothermophilus* PcrA are 3′ to 5′ DNA helicases belonging to the SF1 superfamily and share extensive sequence similarity[6] as well as high structural homology.[6–8] Both Rep and PcrA consist of four major domains called 1A, 2A, 1B and 2B (Figure 1). Crystal structures of Rep bound to ssDNA show two dramatically different Rep monomer conformations ("open" and "closed") that differ from each other by a large reorientation (130° swiveling) of the 2B domain while the other domains remain essentially unchanged (Figure 1a). The crystal structure of a PcrA monomer in complex with a partial duplex DNA (dsDNA with a short 3′ oligodeoxynucleotide tail) is found in the closed form while the structure of a PcrA monomer alone is in the open form. Since both Rep and PcrA crystals were formed at high salt concentrations, conditions under which DNA unwinding is not favored *in vitro*, and because crystal packing could affect the orientation of the highly flexible 2B domain, it is not clear *a priori* whether a single conformation of the 2B domain occurs under solution conditions that support DNA unwinding, or whether both conformations are accessible.

Both Rep and UvrD require more than a monomer to initiate DNA unwinding *in vitro*.[1,2,9] Yet, monomers of both Rep and UvrD are able to translocate along ssDNA with a directional bias (3′ to 5′) (C. Fischer and T. M. L. *et al*., unpublished results), similarly to what has been shown for PcrA monomers.[10,11] In both open and closed forms in the Rep crystal structures,[6] the 3′ end of ssDNA is oriented toward the 1A and 1B domains while the 5′ end is oriented towards the 2A domain (Figure 1b). The same orientation for the 3′ ssDNA tail is observed in the complex of a PcrA monomer bound to a ss/ds DNA.[7] Thus far, the precise DNA-binding orientation in solution has not been determined for any non-hexameric helicase.

In order to detect structural changes of the enzyme and enzyme–DNA complex directly, fluorescent probes can be attached to the protein site-specifically. Measurements using fluorescently labeled helicases have been reported for the *E. coli* DnaB, a hexameric helicase.[12] The Rep helicase is a good model system for this type of fluorescence study since (i) its crystal structure is known, allowing the rational choice of labeling sites, (ii) extensive biochemical information is available,[3] (iii) it can bind to DNA as a monomer, thus simplifying the interpretation of FRET data, and (iv) none of the five native cysteine residues are essential. Our goal is to combine site-directed mutagenesis and ensemble and single-molecule fluorescence analysis, leveraged by the crystallographic structural information, to lay a solid foundation for exploring the structural transitions of protein–DNA complexes.

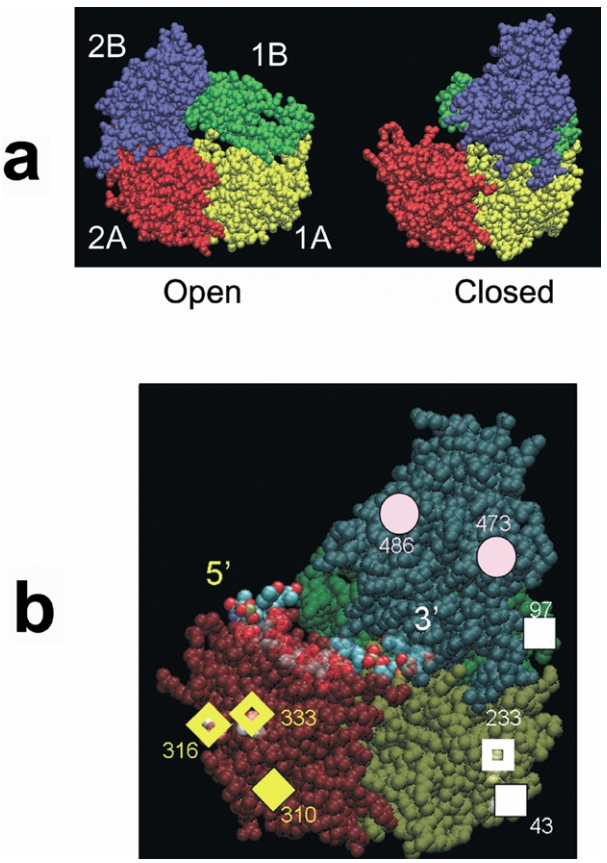

Figure 1. Rep–ssDNA structure and fluorescent labeling sites. a, Rep structures in the open and closed forms. The four sub-domains of the Rep protein are colored as follows. 1A (residues 1–84, 198–275) in yellow, 1B (residues 85–197) in green, 2A (residues 276–373, 544–) in red, and 2B (residues 374–543) in blue. b, The residues on the Rep protein used for site-specific labeling are indicated on the Rep monomer structure in the closed form bound to a ssDNA (each Cys-light mutant has only one cysteine at one of the eight sites shown). The sites are marked with filled symbols if visible in the view and with open symbols if invisible. Circles indicate sites on the 2B domain (473 and 486), squares are sites predicted to be closer to the 3′ end of the ssDNA (43, 97 and 233), and diamonds are sites predicted to be closer to the 5′ end of the ssDNA, hence to the partial duplex junction (310, 316 and 333). Oligo-dT (only nine out of 16 bases in the crystal structure) is shown in a space-filling model and its polarity (3′ *versus* 5′ ends) is marked.

Results

Choice of protein labeling sites

The sites on the Rep protein chosen for site-directed mutagenesis were alanine or serine residues that are not conserved among Rep, UvrD and PcrA, that are not contained within the known helicase motifs, and that are well-exposed on the surface of the protein. Eight labeling sites were chosen (Figure 1), distributed strategically among all four sub-domains, two on domain 1A, one on domain 1B, three on domain 2A, and two on domain 2B. Based on the Rep crystal structure in complex with $(dT)_{16}$,[6] three of these sites are predicted to be closer to the 3′ end of the ssDNA (47, 97 and 233), while three others are predicted to be closer to the 5′ end of the ssDNA (310, 316, and 333), and thus also predicted to be closer to the partial duplex junction of the DNA used in the present studies. The two sites on the flexible 2B domain (473 and 486) were also chosen to deduce the orientation of the 2B sub-domain relative to both the DNA as well as the remainder of the Rep protein (open or closed).

Cys-light Rep mutants retain helicase activity *in vivo* and *in vitro*

The site-directed mutants of Rep in which all of the native Cys residues have been replaced and a single Cys residue has been introduced to a specific position, referred to as Cys-light mutants, could be over-expressed in *E. coli* and were found in the soluble fraction. Western blot analysis was used to confirm that the expressed protein is the Rep protein. Since *E. coli* Rep helicase is the only *E. coli* helicase that can support ϕX174 phage replication,[13] we used plaque assays with ϕX174 phage in an *E. coli* strain that has a deletion for the wild-type *rep* gene and showed that all of these Rep mutants can support ϕX174 phage replication, and thus are active *in vivo*. Our labeling and purification scheme resulted in highly pure preparations of all Rep mutants as checked by SDS-polyacrylamide gel electrophoresis of the labeled mutants. The ssDNA ($(dT)_{70}$)-stimulated steady-state ATPase activity was reduced by only 25% for the labeled mutants (70 ATP hydrolyzed per Rep per second for the wild-type and 50 ATP hydrolyzed per Rep per second for mutants). In addition, the multiple turnover DNA unwinding activities of the unlabeled Rep mutants, measured *via* fluorescence using an 18 bp duplex containing a 3′ $(dT)_{20}$ tail (labeled by Cy3 and Cy5 at the junction),[2] were within 15% of the value obtained with wild-type Rep. Although under the steady-state unwinding conditions used the initiation rate rather than the actual unwinding rate is rate-limiting, we conclude that the steady-state ATPase and DNA unwinding activities of the Cys-light Rep proteins are very similar to those of wild-type Rep.

Fluorescent labeling and purification are streamlined and efficient

Labeling of the Cys-light proteins with fluorophores was performed while they were still bound to a Ni-NTA column. After the labeling reaction, any free fluorophores were removed *via* extensive washing of the column with buffer A (50 mM Tris (pH 8.0 at 4 °C), 150 mM NaCl, 25% (v/v) glycerol). Additional removal of any remaining free fluorophores was achieved by a subsequent purification step using a ssDNA–cellulose column. The labeling efficiencies were determined by comparing the protein absorbance at 280 nm (extinction coefficient of Rep $\epsilon = 76,800\ M^{-1}\ cm^{-1}$) with the absorbance of the fluorophores at their respective absorption maxima (extinction coefficients of Cy3 at 544 nm and Cy5 at 647 nm are $150{,}000\ M^{-1}\ cm^{-1}$ and $250{,}000\ M^{-1}\ cm^{-1}$, respectively), after correcting for the UV absorbance contributed by the fluorophores at 280 nm. The labeling efficiencies ranged from 85% to 95% with the average being 90%. The site-specificity of labeling was at least 90% because control reactions with Cys-free protein show labeling efficiency below 10%. The single-molecule measurements described below further demonstrate that the labeling is highly specific for the single cysteine residues.

Ensemble solution experiments to determine the orientational bias of labeled Rep protein when bound to a partial duplex DNA

To test the binding of labeled Rep proteins to our standard DNA substrate used for helicase studies (an 18 bp duplex with a 3′ ssDNA tail composed of $(dT)_{19}$ or $(dT)_{20}$; Figure 2), we performed bulk solution titrations in which acceptor (Cy5)-labeled Rep protein was added in 1 nM (or smaller) increments to a 5 nM solution of the donor (Cy3)-labeled DNA. As shown in Figure 2a, upon addition of protein, the acceptor signal on the protein increased while the donor signal on the DNA decreased. The apparent FRET efficiency, calculated as the ratio of the acceptor peak intensity and the sum of the peak intensities of the donor and acceptor, increased with increasing protein concentration and reached saturation at similar protein concentrations for Rep protein labeled at each of the three protein labeling sites (43, 333, and 473). Fitting the titration curves using a 1:1 single-site binding model (Materials and Methods) yielded apparent equilibrium-binding constants of 3.6(±0.2) nM for Rep protein binding to DNA in which the donor was at the end of the ssDNA tail (Figure 2b) and 5.0(±0.3) nM for DNA in which the donor was at the ss/duplex DNA junction (Figure 2c). Therefore the observed fluorescence signal changes arise from Rep binding to the DNA. The binding affinity in the low nanomolar range is consistent with our previous single-molecule measurements of Rep monomer binding to a partial duplex DNA.[2] We conclude that the

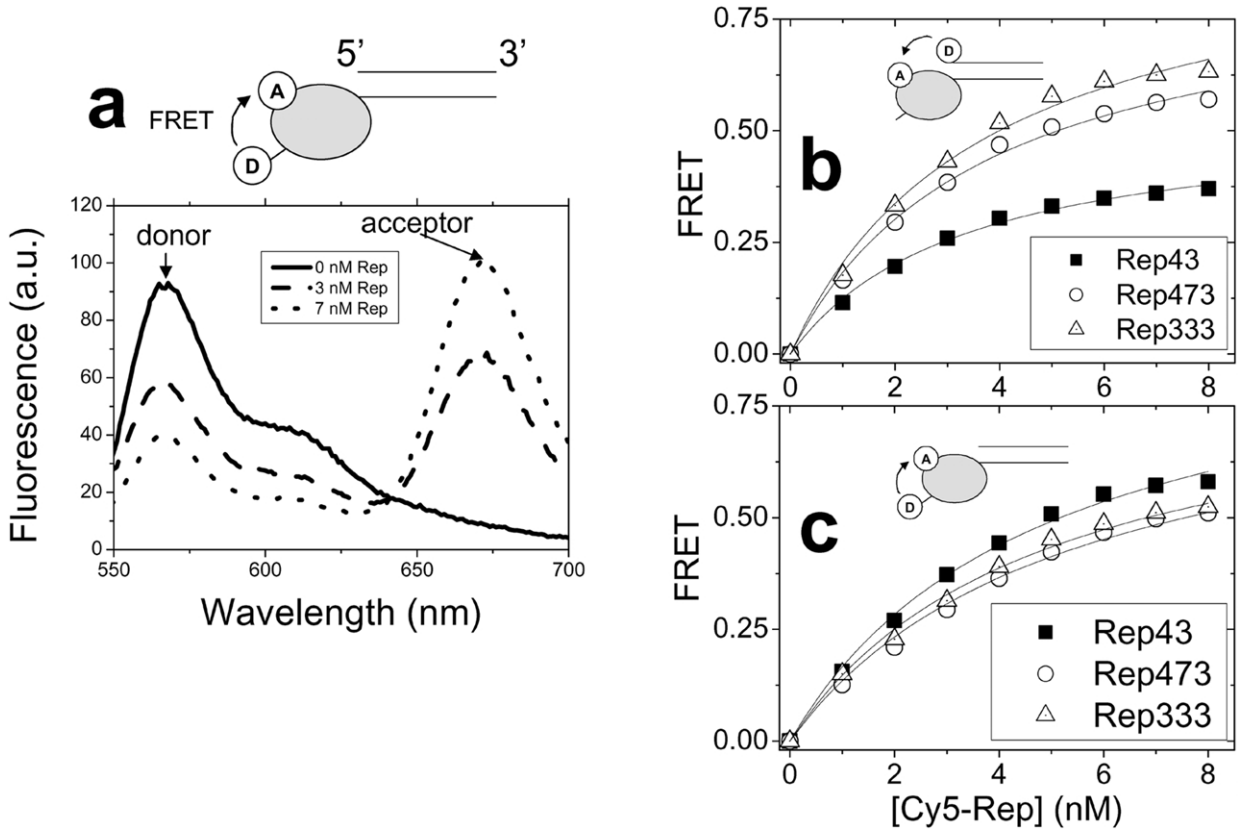

Figure 2. Ensemble FRET studies of fluorescent Rep monomer binding to a fluorescently labeled partial duplex DNA. a, Fluorescence emission spectra are shown for a partial duplex DNA with Cy3 donor labeled at the 3′ end of the $(dT)_{20}$ ssDNA tail (Cy3-DNA) at 5 nM concentration in buffer A and in the presence of 3 nM and 7 nM acceptor-labeled Rep protein (Cy5-Rep43: Rep with single cysteine at 43 position and labeled with Cy5). As Cy5-Rep43 is added to the Cy3-DNA, the fluorescence emission peak of the donor near 565 nm decreases while the acceptor peak near 668 nm increases. Accompanying cartoons illustrate the donor (D), either at the partial duplex junction or at the end of the 3′ ssDNA tail, and the acceptor (A) on the Rep protein (shaded oval). b, Results of equilibrium titrations of a partial duplex DNA with a Cy3 donor label (D) at the ss/duplex junction with Rep labeled with Cy5 (A) at a lone Cys at residue 43, 33 or 473. Apparent FRET efficiency is plotted *versus* [Cy5-Rep] for the three different protein labeling sites. The continuous curves show the non-linear least squares fits of these data to a one-site binding model. c, Apparent FRET efficiency *versus* [Cy5-Rep] for equilibrium titrations of a partial duplex DNA with a Cy3 (D) label attached to the end of 3′ ssDNA tail. The same three Cy5-labeled Rep proteins described in (b) were used for these titrations. The continuous curves show the non-linear least squares fits of these data to a one-site binding model.

DNA-binding properties of Rep are not significantly affected by the mutagenesis or fluorescent labeling.

The apparent FRET efficiency observed at saturating protein concentrations varies among the Rep proteins with Cy5 at the different positions. In particular, Rep with Cy5 at residue 43 shows higher FRET than Rep with Cy5 at residue 333, when the Cy3 donor is at the end of the 3′ ssDNA tail, whereas the reverse is true if the Cy3 donor is placed at the ss/duplex DNA junction. The relative differences in the FRET values among the experiments performed with fluorophores located at different positions on either the protein and/or the DNA are quite clear and were reproducible for two or more independent preparations of labeled proteins. These data suggest that residue 43 is closer to the 3′ end of the ssDNA tail while residue 333 is closer to the ss/duplex DNA junction. We therefore conclude that Rep binds to a ss/duplex DNA in solution with a bias toward the orientation observed in the X-ray crystallographic structures.[6,7]

However, it is difficult to obtain absolute FRET efficiencies from bulk solution measurements due to the likelihood of incomplete labeling and the presence of inactive acceptor species as well as the possibility of multiple-binding stoichiometries. Furthermore, the steady-state bulk solution measurements here do not provide information on the magnitude of the orientational bias. For example, if the protein binds 30% of the time with the reverse orientation, we would not be able to detect the minority species in a steady-state ensemble FRET measurement unless FRET values of these species are known *a priori*. We also note that the gel-FRET technique,[14] in which FRET is measured after electrophoretic separation of the desired complexes, is not applicable here because the Rep–DNA complexes dissociate with a half-life of ~100 seconds (data not shown), which is

far shorter than the time required for gel-electrophoresis. We have therefore used single-molecule FRET measurements to overcome these difficulties. Such measurements can probe fully labeled monomer–DNA complexes in less than one second.

Fluorescently labeled Rep protein binds specifically to DNA, not to the PEG surface

Surface immobilization of the DNA allows a single-molecule observation to be made for extended times, allowing access to dynamic processes that might not be observed otherwise. However, a fundamental problem to be addressed is how to avoid perturbations to the system resulting from surface immobilization. In particular, DNA-binding proteins that are basic may interact strongly with the negatively charged quartz surface. To avoid this, we have used a poly-ethylene glycol (PEG)-coated surface, which has been shown to reject the non-specific surface adsorption of proteins if it forms a dense coating.[2,15,16] Our PEG surface includes a small fraction of PEG molecules possessing end-modified biotin, thereby

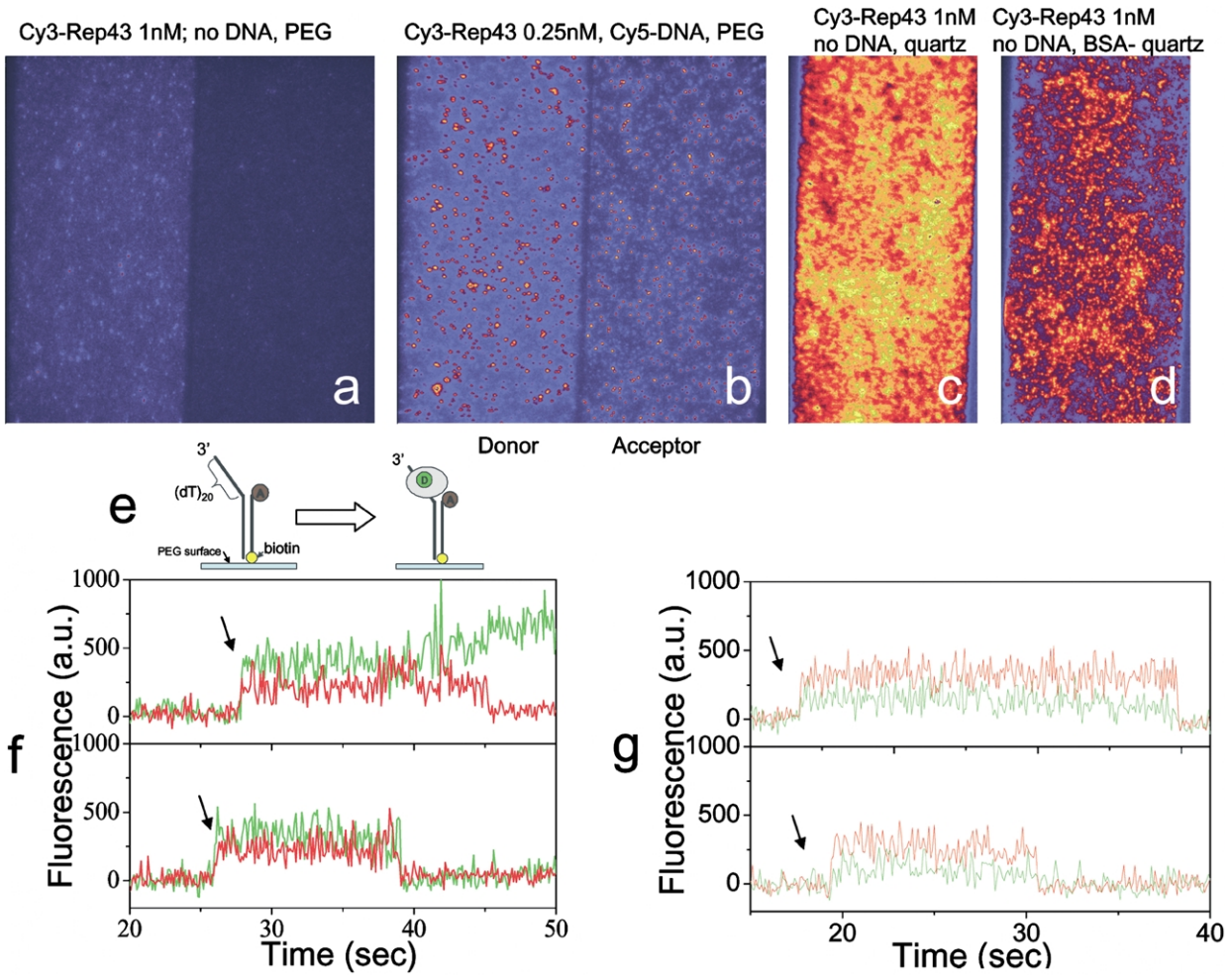

Figure 3. Fluorescently labeled Rep protein binds specifically to DNA substrates attached to a PEG surface. a, Images of donor and acceptor channels show that non-specific binding of Rep protein (labeled with Cy3 donor at residue 43) to the PEG surface is negligible. Only weakly fluorescent impurities, with less than a third of the intensity of the fluorophores conjugated to the protein, are visible. b, Donor-labeled proteins bind efficiently to Cy5-acceptor-labeled DNA molecules immobilized to the surface as shown schematically in (e), giving rise to hundreds of fluorescent spots in both imaging channels. c, A donor channel image showing the result of non-specific binding of Cy3-donor-labeled Rep to a bare quartz surface. d, A donor channel image showing the non-specific binding of donor-labeled proteins to a BSA-coated quartz surface. e, Schematic illustration of single-molecule binding of a donor-labeled Rep protein to an acceptor-labeled DNA immobilized to a PEG surface. f, Examples of single-molecule binding events measured with Cy3-labeled Rep (1 nM) (labeled at a single Cys at position 43). Red and green curves represent the signals of acceptor and donor, respectively. g, Examples of single-molecule binding events measured with Cy3-labeled Rep (1 nM) (labeled at a single Cys at position 333). No signal is detected before Rep binding because direct excitation of the Cy5 acceptor is insignificant at the excitation wavelength used (532 nm) and Cy3 donor-labeled Rep protein diffusing in solution contributes only to the background counts. Upon protein binding to the DNA, fluorescence signals appear abruptly (marked by arrows). After the binding, either (i) the acceptor photobleaches, leading to donor signal increase (top graph in (f)), or (ii) total signal disappears abruptly (bottom graph in (f) and top and bottom graphs in (g)).

allowing specific immobilization of a biotinylated DNA molecule while minimizing non-specific adsorption of protein to the underlying surface.

The single-molecule FRET measurements were performed as follows. (1) The streptavidin-coated PEG surface was prepared. (2) 1 nM donor-labeled Rep protein in imaging buffer was added to the sample to test for non-specific binding. Typically less than ten fluorescent spots appeared in the 50 μm × 100 μm imaging area in the absence of DNA (Figure 3a). (3) Biotinylated, acceptor-labeled DNA (10–100 pM in 10 mM Tris–HCl (pH 8.0), 50 mM NaCl, 0.1 mg/ml BSA) was added. No DNA binding was observed if the DNA lacked biotin or if streptavidin was omitted. (4) 0.25–1 nM donor-labeled Rep in the imaging buffer was added, resulting in hundreds of fluorescent spots in both donor and acceptor channels (Figure 3b). Movies of 5–60 seconds duration were obtained at ten frames per second and analyzed to obtain the time records of donor and acceptor fluorescence signals of individual molecules.

On the PEG surfaces, at least 95% of the Rep protein binding events were due to specific binding to the DNA (see below). In contrast, the addition of a 1 nM solution of the labeled Rep to a bare quartz surface (Figure 3c) or a BSA-coated surface (Figure 3d) resulted in very high degrees of non-specific surface binding so that single molecules could not be discerned as isolated spots. It was therefore essential to use the PEG surface for our studies.

Direct observation of a single Rep monomer binding to DNA

For single-molecule measurements, the protein was labeled with Cy3 (donor) and the DNA was labeled with Cy5 (acceptor). This allows us to easily distinguish a single monomer-binding event from multiple monomer binding events. When a protein binds to a DNA molecule in the middle of a time record (illustrated in Figure 3e), a sudden appearance of fluorescence signals is observed (Figure 3f and g). On the average, about half the binding events showed the donor-only signals while the other half showed both the donor and acceptor signals. It is highly unlikely that the binding events showing FRET are due to non-specific binding to the PEG surface, since the probability that random binding of protein to the surface would occur within a 10 nm radius of an acceptor-labeled DNA is ~0.001% for the typical surface densities of DNA used. Control experiments without DNA showed a much reduced-binding frequency (Figure 3a). In addition, a large fraction of the donor-only binding events are likely due to fluorescently inactive acceptor species as has been commonly observed in single-molecule FRET experiments.[17] Therefore, we conclude that the vast majority of the protein-binding events are specific to DNA.

After the initial-binding event, one of two results followed. Either (i), the acceptor underwent photobleaching, leading to an increase in donor signal (top panel in Figure 3f), or (ii), the total signal disappeared abruptly (bottom panel in Figure 3f and top and bottom panels in Figure 3g). The average time until the disappearance of the total signal was reduced at higher laser intensities and an independent measurement showed that dissociation of Rep–DNA complexes is substantially slower (~$0.01\ s^{-1}$) than the rate of loss of the total signal. Therefore, it is likely that the observations of a loss of total signal are due to photobleaching of the donor fluorophore. At least 95% of the donor photobleaching events were single-stepped, consistent with the signal originating from a single fluorophore event. Since the labeling efficiency of the Rep protein is high (~90%), this suggests that Rep binds to the DNA predominantly as a monomer under these conditions. This also indicates that the probability of having more than one fluorophore attached to a single protein is less than 10%. A similar analysis also showed that over 90% of the Rep protein bound to the DNA at any time is monomeric. These results indicate that reliable studies of Rep monomer binding to a single DNA molecule are possible *via* single-molecule experiments of this type.

Single-molecule measurements suggest that the orientation of Rep binding to the DNA is definitive

The donor and acceptor intensities (I_D and I_A) of individual DNA molecules were obtained by averaging the first ten frames (one second) of time traces after correction for the cross-talk between the two signal channels. Single-molecule FRET efficiency E was calculated as $E = 1/(1 + \eta I_A/I_D)$, where η is a parameter reflecting the relative quantum yields and relative detection efficiencies of the donor and acceptor signals.[18] The value of η was determined experimentally as the ratio between the absolute changes in I_A and I_D upon acceptor photobleaching[18] and is close to 1 in our experimental configurations. Therefore, the single-molecule FRET efficiency E was determined from $E = 1/(1 + I_A/I_D)$, and its histograms are shown in Figure 4 for three protein labeling sites (the donor at 43, 333, and 473) and two DNA labeling sites (the acceptor at the end of the ssDNA tail or at the partial duplex junction).

Approximately, half of the population of DNA molecules was observed to cluster in a peak centered at $E \sim 0$, representing the donor-only species likely due to the population of molecules whose Cy5 acceptor on the DNA is inactive. Negative values of E arise from signal fluctuations at the acceptor channel near the background level. The acceptor-labeled DNA molecules are not detectable by themselves since the absorbance of Cy5 at the excitation wavelength (532 nm) is approximately 25 times lower than its peak absorption. Each single-molecule FRET histogram in Figure 4 also shows an additional peak centered at a non-zero

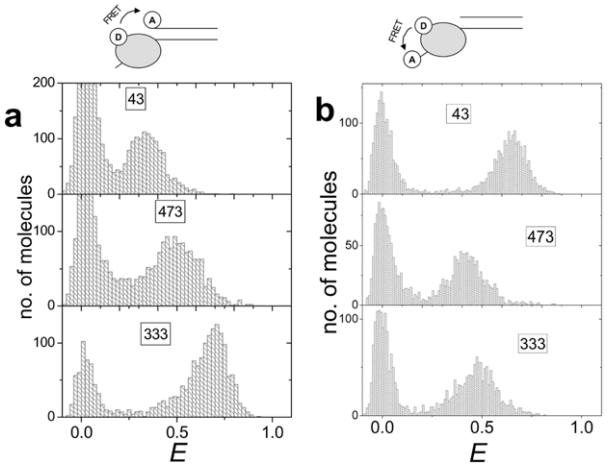

Figure 4. Single-molecule FRET studies of fluorescently labeled Rep monomer binding to fluorescently labeled DNA to determine the orientation of Rep bound to the DNA. FRET efficiency between a single Cy3-labeled Rep and a Cy5-labeled DNA was obtained by averaging their fluorescence signals over one second (ten frames of 0.1 second duration). Histograms of single-molecule FRET values were constructed from hundreds of molecules for each condition. a, Cy3-Rep (labeled on single Cys at positions 43, 473 and 333) binding to DNA with Cy5 at the partial duplex junction. b, Cy3-Rep (labeled on a single Cys at positions 43, 473 and 333) binding to DNA with Cy5 at the 3′ end of the ssDNA tail. Each histogram shows two peaks; the peak at zero FRET is attributed to donor-only cases (likely Cy3 labeled Rep bound to DNA without an active Cy5). Negative FRET values are caused by noise and background subtraction and the fact that the acceptor signal is at the background level. The non-zero peaks of FRET efficiencies show clear differences dependent upon the site of Cy3 (acceptor) labeling on Rep protein as well as the site of Cy5 (donor) labeling on the DNA. The relative FRET values are consistent with the results of the bulk solution measurements shown in Figure 3.

value of E that arises from a Rep monomer binding to a DNA. The positions of the peaks are clearly different for the different labeling sites and these relative differences in peak position were reproducible over independent surface preparations and independent preparations of labeled proteins. Furthermore, these differences in peak positions among the different labeling sites are fully consistent with the bulk solution measurements shown in Figure 2. We also note that single FRET peaks are observed from each histogram without additional peaks that might occur if the reverse-binding orientation is significantly populated. This suggests that the fluorescent labeling is highly site-specific and DNA binding occurs with a definite polarity.

The width of the peaks in the histograms can arise from several sources. At the instrumental level, uneven sensitivity of different areas of the camera, imperfect mathematical mapping between two images (donor and acceptor channels), and intensifier noise are among the possible sources. Statistical noise due to the limited number of photons can also be significant in single-molecule measurements. Heterogeneities in the spectral properties, quantum yields, and dipole orientations of the fluorophores can also contribute to the width. At the molecular level, the presence of several alternative protein-binding sites on the DNA is another possible source. Since Rep can bind non-specifically to both ssDNA and duplex DNA, but with higher affinity to ssDNA, there are multiple potential non-specific-binding sites for a Rep monomer on the 3′-$(dT)_{20}$ ssDNA region of the DNA substrate. It is also possible that the Rep–DNA complex can exhibit multiple conformations that can be manifested in the broadening of the FRET distribution or in the asymmetric peaks seen in some cases. Finally, some of the aforementioned possible sources of noise may be affected by the exact configuration in which a Rep–DNA complex interacts with the local environment of the surface. Here, we do not attempt to de-convolute the relative contributions of these potential sources. Instead, we focus on the average values of E determined by Gaussian fitting of the peaks in the histograms.

Binding orientation information is independent of the type of fluorophores used

In principle, the spectral properties or orientations of the fluorophores in the labeled Rep

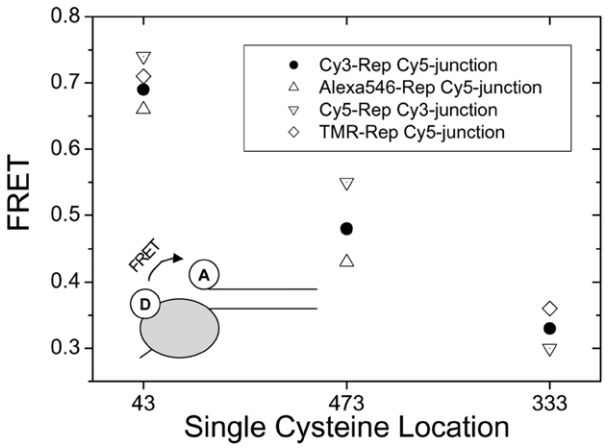

Figure 5. The relative changes in FRET values among labeling sites are independent of the FRET pair used. To test the effect of the particular FRET pair on the robustness of the dependence of the FRET values on the position of the Rep protein labeling sites, we tested the following different FRET pairs. (i) One of three different donors (Cy3, Alexa555, or tetramethylrhodamine) was attached to the protein with Cy5 as the acceptor on the DNA. (ii) The Cy3 donor and Cy5 acceptor locations were switched (i.e. Cy3 was placed on the DNA and Cy5 on the protein). Average FRET values were obtained by fitting the non-zero FRET peaks as shown in Figure 4 using Gaussian functions. The scatter of the FRET values for each protein labeling site is significantly smaller than between sites, independent of the FRET pair used.

protein could be influenced by the local environment of each labeling site and this could lead to apparent variations in FRET efficiencies among the different sites, for instance due to effects involving differences in κ^2. In order to test the robustness of the binding orientation information, we switched the locations of the donor and acceptor fluorophores (i.e. placed the Cy3 donor on the DNA and the Cy5 acceptor on the Rep), and also replaced the Cy3 donor with other fluorophores possessing similar spectral properties (e.g. Alexa555 and tetramethylrhodamine). Although the absolute values of the FRET efficiencies, E, varied slightly among the different fluorophore combinations, each protein labeling site displayed a distinct clustering of the values of E, independent of the fluorophore (Figure 5). In addition, the monotonic decrease in FRET when the labeling site is moved from residue 43 to 473 and then to residue 333 is observed for all fluorophore combinations (Figure 5). This result strongly supports the conclusion that the differences in FRET observed for the different labeling sites reflect the relative changes in distance between sites on the protein and the DNA due to the unique binding orientation of a Rep monomer on the DNA, rather than effects due to specific changes in the properties of the fluorophores themselves that are dependent on the labeling site.

Triangulation shows that Rep bound to a partial DNA duplex is in the closed form

To obtain more detailed information on the binding geometry between Rep and DNA, we performed additional single-molecule FRET experiments. In these experiments, Rep monomers were labeled with Cy3 at each of the eight labeling sites on the protein, as shown in Figure 1b (eight distinct Rep proteins with one cysteine at each of the eight positions) and the DNA was labeled with Cy5 at the ss/duplex DNA junction. The resulting average FRET values, widths of the FRET peaks in the histograms as well as the fluorescence quantum yields of each Cy3 donor and fluorescence polarization anisotropy are presented in Table 1.

Table 1. Single molecule FRET analysis of Rep–DNA complex

Cy3 labeling site	FRET to Cy5 at the junction	Width	Quantum yield (%)	Fluorescence anisotropy
43	0.33	0.19	39	0.19
97	0.38	0.3	37	0.3
233	0.31	0.27	47	0.27
310	0.55	0.24	48	0.24
316	0.58	0.3	40	0.3
333	0.68	0.17	41	0.17
473	0.47	0.31	31	0.31
486	0.71	0.23	31	0.23

FRET histograms for the eight different protein sites as shown in Figure 5 were fitted using Gaussian functions and the values for the center and width are listed. Also shown are the values for the quantum yield and fluorescence anisotropy of Cy3 attached to the protein.

Using these data, we wished to determine whether the Rep monomer was bound to the ss/duplex DNA principally in either the open or closed conformation. To estimate the location of the partial duplex junction we performed the following triangulation procedure.

(1) To account for the flexible fluorophore linker, we assumed that the donor fluorophore on the protein is displaced from the corresponding Cys residue by 5 Å in the direction moving away from the protein center. Residue locations were obtained from the structural coordinate file (Protein Data Bank Id: 1uaa).

(2) We used a biased random walk of the junction location $\vec{r}$ to minimize the function $\Pi = \sum_i (E_i - E_{\mathrm{cal},i})^2$ where E_i is the experimentally determined FRET efficiency for residue i and

$$E_{\mathrm{cal},i} = \left[1 + \left(\frac{|\vec{r} - \vec{r}_i|}{R_{0,i}}\right)^6\right]^{-1}$$

is the calculated FRET efficiency between the acceptor fluorophore (Cy5) at the junction location ($\vec{r}$) and the donor fluorophore (Cy3) at the residue i on the protein ($\vec{r}_i$). $R_{0,i}$ is the Förster radius calculated for residue i, which ranged between 61 and 65 Å (see Materials and Methods). Three-dimensional biased random walks of $\vec{r}$ with a step size of 0.5 Å were performed using MATLAB to minimize Π, starting from random initial positions chosen within a 200 Å^3 volume surrounding the protein. Approximately, half of the trajectories were trapped in local minima and only the trajectories that resulted in the global minimum were considered. Averaging ten such runs yielded an estimate for the location of the acceptor, and thus also for the junction.

We first assumed that the Rep monomer was bound in the closed conformation and used the crystal structure of the closed form of Rep to predict the position of the Cy5 on the DNA substrate. For the closed form of Rep, triangulations using all eight constraints (two from 1A, one from 1B, three from 2A and two from 2B) yielded the Cy5 location shown in Figure 6. The model is well defined because the standard deviation about the mean position is only 0.9 Å for ten runs. The same triangulation process but using only six constraints (excluding the two constraints from the fluorophores within the 2B domain) gave a mean Cy5 acceptor location that was displaced only by 5.5 Å. If instead, we assume that Rep was bound to the DNA in the open conformation, then the predicted Cy5 acceptor location estimated using all eight constraints differs by 66 Å from that estimated using the six none-2B constraints. These results are therefore consistent with the Rep monomer

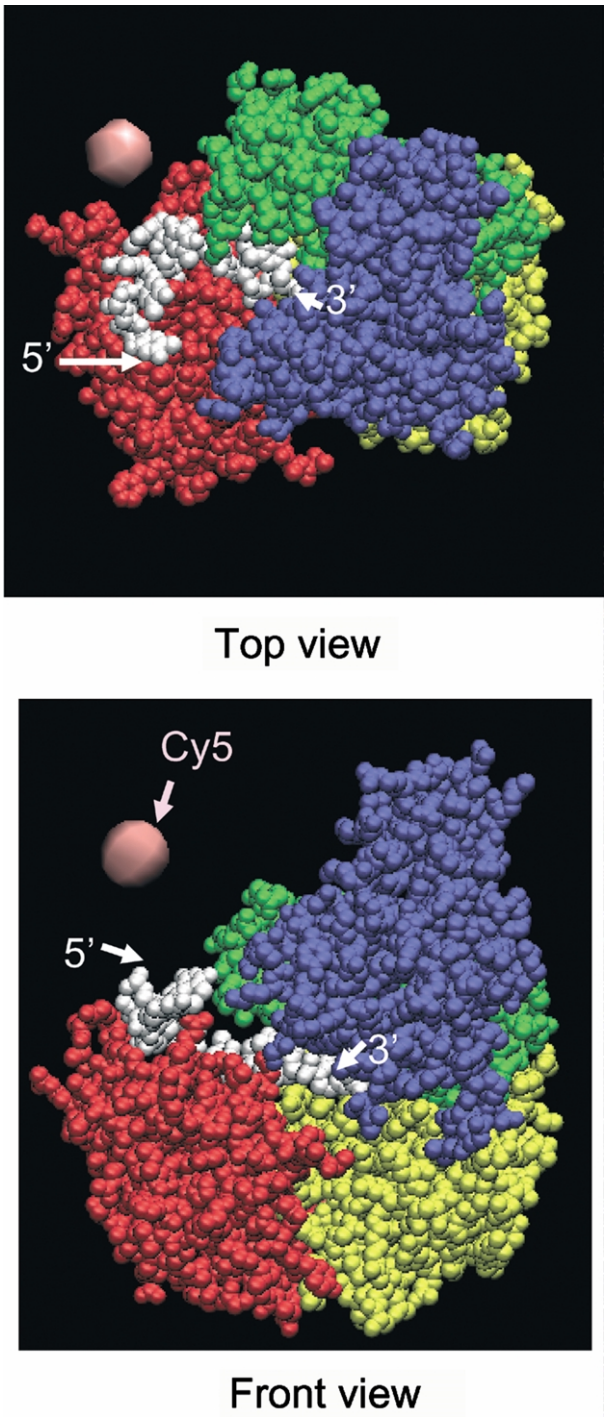

Figure 6. Position of the partial duplex junction relative to the Rep structure. Two views, rotated 90 degrees relative to each other, are shown of the closed form of the Rep monomer bound to ssDNA (from the Rep–ssDNA crystal structure) indicating the location of the Cy5 acceptor (red dot) that is attached to the ss/dsDNA junction of the partial DNA duplex, as estimated from the triangulation procedures described in the text.

being bound to the DNA in the closed form and inconsistent with the open form.

Based on these measurements and calculations, it appears that Rep monomer exists in a conformation more similar to the closed form than to the open form when it is bound to a DNA unwinding substrate in solution *in vitro*. We also note that these conclusions are insensitive to the values used for parameters such as linker length (5 Å *versus* 10 Å) and R_0 values except for slight changes in the numeric values above. However, we cannot rule out minority populations (<10%) of the open conformation or other conformations that may differ from the crystal structures, since the triangulation procedure is not sensitive to the presence of such small populations.

Discussion

Quantitative FRET measurements can be used to build models of macromolecular complexes through triangulation procedures.[19] Single-molecule measurements are useful for the quantitative determination of FRET efficiencies because multiple species may exist in bulk solution measurements, which can complicate the analysis.[17,20,21] Furthermore, gel FRET methods[14] that measure FRET after electrophoretic separation of the desired complexes are not practical if the complex dissociates on a time scale shorter than that of the electrophoresis experiment.

In order to observe single-molecule fluorescence signals through extended periods of time, it is necessary to immobilize the molecules while preserving their biological activity. Previously, we have shown that the use of a PEG surface coating efficiently prevents non-specific interactions of DNA and proteins with quartz surfaces, thereby reproducing bulk solution kinetics.[2] Here, we have directly shown that fluorescently labeled proteins do not adsorb to the PEG surface even though they strongly bind non-specifically to untreated or BSA-coated quartz surfaces. DNA immobilization does not appear to affect Rep's ability to bind to the DNA with a proper orientation because the relative FRET efficiencies among the different labeling sites determined from the single-molecule studies are fully consistent with bulk solution measurements. Cysteine engineering and fluorescent labeling did not significantly affect the enzymatic activities of Rep as we have tested these both *in vivo* and *in vitro*. Our data also provide direct evidence that at the low nanomolar Rep protein concentrations used, most of the binding events to the $(dT)_{20}$-tailed DNA reflect individual Rep monomers rather than multiple monomers binding to the same DNA. This is consistent with previous studies, which indicated that an occluded region on a ssDNA by high-affinity binding of Rep is approximately 15 nucleotides[22] and our single-molecule studies which indicated that only a monomer binds to the DNA at low nanomolar concentrations.[2]

In the use of FRET measurements to estimate distances between fluorophores bound to biomolecules, the most significant unknown is the orientational factor, κ^2. In the triangulation procedures

used to determine whether the 2B domain is in the open or closed conformation, we assumed that $\kappa^2 = 2/3$. This is clearly a crude approximation since the fluorophores displayed relatively large fluorescence anisotropy and the assumption of $\kappa^2 = 2/3$ is strictly valid only if both fluorophores are rotating freely relative to the host molecule within their fluorescence lifetimes. Nevertheless, dipole orientations are not expected to be a major concern in this study that used eight different constraints since such over-sampling would reduce the contributions of potential errors that arise from the orientational effects. The fact that we obtained consistent results for various fluorophore combinations also suggests that the information obtained here is robust regardless of how a particular fluorophore interacts with the DNA or protein.

Our studies indicate that a Rep monomer binds to ssDNA with a definite polarity in solution. Previous fluorescence studies have shown that a Rep monomer binds to ssDNA with a directional bias but the binding orientation could not be determined since only a single probe was used.[23] All three protein–DNA crystal structures (two for Rep,[6] one for PcrA[7]) indicate the same binding orientation for the ssDNA. Our ensemble FRET data show that there is an orientational bias in DNA binding consistent with the crystal structures. Single-molecule FRET data show that the bias is very strong and, within our resolution, the protein binds to the DNA with a definitive polarity. Similar measurements using single-stranded DNA in bulk solution indicate that the same orientational bias is maintained (data not shown); hence the binding orientation is unlikely to be influenced by the presence of the duplex.

Crystal structures of the Rep protein bound to ssDNA ($(dT)_{16}$) show the Rep monomer in two distinct conformations, referred to as closed and open.[6] The two forms differ primarily by a large reorientation (130° swiveling) of the 2B sub-domain about a hinge region connecting it to the 2A subdomain. Rep binding to ssDNA increases the sensitivity of the hinge region to trypsin cleavage, suggesting that some movement of the 2B subdomain is coupled to ssDNA binding.[24] The open form of Rep has its sub-domains arranged in a similar configuration as is observed in the crystal structure of the apo PcrA monomer (without DNA),[8] whereas the closed form of Rep more closely resembles the form of PcrA observed in the crystal structure of a complex with a partial duplex DNA.[7] The studies reported here were designed to test if a Rep monomer binds to a partial duplex DNA in a unique conformation (closed or open) or whether it can sample many conformations.

The triangulation procedures that were based on six or eight distance constraints allowed us to deduce the average location of the fluorophore attached to the DNA junction with respect to the site-specific fluorophores on the bound Rep protein. The estimated location of the partial duplex junction is in the general vicinity of the junction seen in the PcrA structure, although the agreement is not exact. If the partial duplex junction bound to Rep were positioned as in the PcrA crystal structure, this would predict a near 100% FRET signal when Cy3 donors are attached to residues 310, 316 and 333, whereas we observed much smaller values of FRET. This difference suggests that a Rep monomer does not bind precisely at the junction for the ssDNA tail lengths used in our experiments. This might arise from the difference in the lengths of the ssDNA tails used in the two studies. In contrast to the $(dT)_{20}$ tail used in our studies, the DNA in the PcrA structure had only a $(dT)_7$ ssDNA tail, which would be expected to constrain the protein to bind closer to the partial duplex junction. In contrast, Rep does not show specificity for binding to the ss/duplex DNA junction[1] and thus Rep would be expected to sample the multiple binding sites available along the ssDNA tail. If this is the case, then the junction location estimated in our studies should be viewed as an average over these multiple binding sites.

Performing the triangulation procedures for both closed and open forms as they appear in the Rep crystal structures allowed us to deduce that the conformation of a Rep monomer bound to the DNA substrate is most similar to the closed form. This represents the first determination of the orientation of the 2B domain for a DNA bound SF1 helicase in solution. Both the Rep and PcrA crystals were formed at much higher salt concentrations (100–150 mM NaCl) than those that favor DNA unwinding *in vitro*, and because crystal packing could affect the orientation of the highly flexible 2B domain, it was not *a priori* clear which conformation would be preferred under solution conditions that support DNA unwinding. However, it is important to note that a Rep monomer is unable to initiate[1] or sustain DNA unwinding *in vitro*.[2] Rather, Rep must oligomerize in order to initiate DNA unwinding *in vitro*.[1] Since we used the same solution conditions as in the previous Rep–DNA unwinding experiments,[1,2] the 2B domain orientation that we determined here corresponds to the conformation of a Rep monomer bound to a partial duplex DNA in the absence of ATP. This would be the typical initial state that exists in single-turnover DNA unwinding kinetics experiments when the DNA substrate is in excess over the Rep protein. However, under these conditions, single-turnover DNA unwinding experiments do not detect even partial unwinding of duplex DNA.[1] Therefore, the closed form of a Rep monomer bound to a partial duplex DNA, which largely resembles the PcrA crystal structure, likely represents an inhibited form of the enzyme.

Recent studies have shown that a Rep deletion mutant that lacks the 2B domain can still function as a helicase, both *in vitro* and *in vivo*,[25] hence the 2B sub-domain is clearly not required for Rep helicase function. In fact, the 2B deletion mutant of Rep is more efficient as a helicase *in vitro* than is

the full length wild-type Rep,[25] suggesting further that the 2B domain has an inhibitory effect on unwinding. An interesting hypothesis then is that the interaction of an additional Rep monomer(s) with the inhibited Rep monomer bound to DNA in the closed form may be necessary to activate the Rep protein to initiate DNA unwinding.[25] Future experiments using doubly labeled Rep proteins may be able to test this hypothesis directly.

Conclusions

We have developed reliable procedures for measuring interactions between the *E. coli* Rep protein and DNA at the single molecule level. The orientation of an SF1 monomer with respect to the DNA backbone polarity has been determined in solution for the first time and the orientation of the flexible 2B domain of Rep has been deduced to be in the closed form when bound to a partial duplex DNA. Future studies of more labeling sites and of doubly labeled proteins at different steps during the ATP hydrolysis cycle should be able to elucidate overall structure changes of the Rep–DNA complex along the reaction pathway.

We anticipate that the approaches outlined here can be used to probe many outstanding questions about helicase mechanisms in general, and Rep helicase in particular. Why do many helicases, including Rep, require oligomerization (dimer, trimer, hexamer,…) to function? What determines the directionality in DNA unwinding and translocation? How does the helicase couple conformational changes induced by ATP hydrolysis for use in DNA unwinding and translocation? Future experiments using fluorescently labeled helicases can be designed to detect conformational changes of the enzyme and DNA unwinding simultaneously from the same molecule, thereby directly probing the heart of the structure–function relationship.

Materials and Methods

Buffers

Lysis buffer is 50 mM Tris (pH 8.0 at 4 °C), 200 mM NaCl, 15% (v/v) glycerol and 20% (w/v) sucrose. Buffer A (for Ni-NTA column) is 50 mM Tris–HCl (pH 8.0 at 4 °C), 150 mM NaCl, 25% glycerol. Buffer B (Ni-NTA elution buffer) is buffer A plus 100 mM imidazole. Buffer C (for ssDNA cellulose column) is 50 mM Tris (pH 7.5 at 4 °C), 100 mM NaCl, 2 mM EDTA, 20% glycerol. Buffer C-1 M (ssDNA–cellulose elution buffer) is buffer C plus 1 M NaCl. Buffer C-3 M (ssDNA–cellulose wash) is buffer C plus 3 M NaCl. The final purified protein was stored in 30 mM Tris (pH 7.5 at 4 °C), 600 mM NaCl, 1.2 mM EDTA, 50% glycerol at −20 °C.

Site-directed mutagenesis

Site-directed mutagenesis was performed using the "QuikChange" technique (Stratagene) on pGG236, a plasmid containing the *rep* gene under control of the *tac* promoter. All five native cysteine residues in the Rep protein were replaced with the indicated amino acids (C18L, C43S, C167V, C178A, C612A) using this approach. Cysteine residues at positions 18 and 167 were changed to leucine and valine (corresponding to the residues found in *E. coli* UvrD and *B. stearothermophilus* PcrA), respectively, because protein solubility was lowered considerably when they were replaced with serine. None of the original cysteine residues in Rep are conserved among Rep, UvrD and PcrA. After each round of mutagenesis, the DNA sequence for the entire Rep gene was confirmed and Rep activity was tested *in vivo* using a plaque assay for ϕX174 phage[25] in an *E. coli* strain CK11Δ*rep*/pIWcI that lacks Rep gene.[26] The open reading frame (ORF) of the cysteine-free mutant was digested with restriction enzymes (*Nde* I and *Xho* I), and ligated into the plasmid pET28a (Novagen) that carries an N-terminal hexa-histidine tag to generate an expression vector. Using this plasmid, pRepNoCys that carries the cysteine-free Rep gene as a background, we made plasmids encoding mutant *rep* genes encoding only a single cysteine residue at eight different positions, pRepS43C, pRepA333C, pRepS316C, pRepA310C, pRepS233C, pRepA97C, pRepA473C, pRepS486C, thereby generating eight different Rep mutants containing only one cysteine residue each.

Protein purification and labeling

The plasmids encoding each Rep mutant were each used to transform BL21(DE3) (Novagen, 69864-3) and colonies were selected on agar plates containing 30 μg/ml kanamycin (Sigma, St Louis, MO). Single colonies were picked and grown overnight at 37 °C in LB broth with kanamycin (30 μg/ml). This culture (1 ml) was used to inoculate 100 ml of fresh LB medium, and incubated at 30 °C. The growth temperature was lowered to 30 °C to improve solubility of the Rep protein. Cell growth was monitored by optical density at 600 nm. When $OD_{600} = 0.8$, expression of the Rep protein was induced by the addition of 300 μM IPTG (isopropyl-β-D-thiogalalctopyranoside). Following induction, the cells were grown for an additional three hours and harvested by centrifugation. The following purification and labeling of the Rep mutants were performed at 4 °C. Cell paste (1 g) was resuspended in 5 ml of lysis buffer. PMSF was added to 0.1 mM and lysozyme to 0.4 mg/ml. After one hour of gentle stirring, the cell suspension was subjected to pulsed sonication on ice for three minutes (70% duty cycle, power setting of 7). The cell lyzate was centrifuged at 14,000 rpm for one hour. The supernatant was mixed with 500 μl of Ni-NTA agarose column (Qiagen) for one hour by gentle stirring at 4 °C. The protein-bound Ni-NTA agarose was then poured into an empty column. The column was washed with 15 column volumes of buffer A. The column was treated with Tris(2-carboxyethyl)phosphine (TCEP) (100 μM) to reduce any disulfide bonds that might have formed. The column was then washed with 15–20 column volumes of buffer A. The appropriate fluorophore (Cy3-maleimide or Cy5-maleimide (Amersham Biosciences, Piscataway, NJ) or Alexa555-maleimide and tetramethylrhodamine-maleimide (Molecular Probes, Eugene, OR)) was then added to the Ni-NTA column at a tenfold molar excess over the protein concentration in buffer A and incubated overnight at 4 °C, while slowly rotating the sample container. Free fluorophores were removed

by washing the column with buffer A (10–15 column volumes). The labeled protein was then eluted from the column with buffer A containing 100 mM immidazole. The eluted protein was loaded onto a single-stranded DNA–cellulose column (USB, Cleveland, Ohio) pre-equilibriated with buffer A and eluted with elution buffer (buffer C-1M). The concentrations of Rep and each fluorophore in the final preparation were determined spectrophotometrically by recording spectra from 240 nm to 700 nm. Spectral readings revealed that the fractions eluted from the Ni-NTA column contained some free fluorophores (5–10%), which were removed by the ss-DNA–cellulose column. The final labeling efficiency was generally above 90%. The protein was stored in 30 mM Tris (pH 7.5 at 4 °C), 600 mM NaCl, 1.2 mM EDTA, 50% glycerol at −20 °C.

Oligonucleotides

Sequences used for binding studies were 5′-Cy5(or Cy3)-GCCTCGCTGCCGTCGCCA-3′-Biotin and 5′-TGG CGACGGCAGCGAGGC$(T)_{20}$-3′ for a partial duplex DNA with the fluorophore at the junction and 5′-GCCT CGCTGCCGTCGCCA-3′-Biotin and 5′-TGGCGACGGC AGCGAGGC$(T)_{19}$ -Cy5(or Cy3)-T-3′ for a partial duplex DNA with the fluorophore at the end of the 3′ end of the single-stranded tail. Bulk unwinding test was done using 5′-Cy5-GCCTCGCTGCCGTCGCCA-3′-Biotin and 5′-TGGCGACGGCAGCGAGGC-Cy3-$(T)_{20}$-3′. Oligonucleotides were synthesized and purified as described.[1] Cy3 and Cy5 were incorporated in phosphoramidite forms and biotin was added as BiotinTEG CPG (all three from Glen Research, Sterling, VA) during automated synthesis. The DNA was gel-purified and annealed in 10–30 μM concentrations in 20 mM Tris–HCl (pH 8.0), 500 mM NaCl.

ATPase assay

Steady-state ATPase activities of Rep mutants and the wild-type were measured using the EnzChek phosphate assay (cat. no. E-6646) (Molecular Probes, Eugene, OR). The kit enables a continuous spectrophotometric monitoring of reactions that generate inorganic phosphate. Each reaction is carried out by mixing DNA substrate ($(dT)_{70}$, 1 μM), MESG (2-amino-6-mercapto-7-methylpurine), buffer U, 1.5 mM ATP, purine nucleoside phosphorylase, and 10–20 nM mutant Rep protein. ATP was added last after incubating the mixture at room temperature for ten minutes. OD at 360 nm (OD_{360}) was monitored for five minutes after addition of ATP. Enzymatic conversion of MESG results in a spectrophotometric shift in the peak of maximum absorbance from 330 nm to 360 nm. The number of ATP molecules hydrolyzed per Rep per unit time is calculated from the initial linear increase in OD_{360}.

Ensemble fluorescence measurements

Ensemble solution measurements were performed using an Eclipse fluorometer (Varian) in buffer U (10 mM Tris–HCl (pH 7.4), 6 mM NaCl, 1.7 mM Mg^{2+}, 10% glycerol, 1% (v/v) beta-mercaptoethanol, 0.1 mg/ml BSA) in a total volume of 1 ml. For FRET measurements, donor-labeled DNA was first added to 5 nM concentration, then acceptor-labeled Rep protein was added at 1 nM (or smaller) increments until saturation. Emission spectra were measured upon excitation at 532 nm and corrected using the pre-determined spectral response function of the fluorometer. The apparent equilibrium-binding constant K_D was estimated by fitting the FRET *versus* [Rep] curve to the following equation, $E_{app} = E_0 + (E_{max} - E_0)[Rep]/([Rep] + K_D)$ where E_{app} is the apparent FRET signal, E_0 is the FRET value in the absence of protein and E_{max} is the FRET value at saturating protein concentrations. Fluorescence anisotropy of protein-conjugated fluorophores was measured using 5 nM solution of labeled proteins. Fluorescence anisotropy of Cy5-labeled DNA was measured in 20 nM solution. The quantum yields of protein-conjugated Cy3 were measured in 5 nM concentration using rhodamine 101 as a standard. Unwinding of 18mer duplex with $(dT)_{20}$ tail was measured *via* FRET with the DNA concentration of 1 nM and 0.5 mM ATP.

Determination of R_0

R_0 is defined according to:[27]

$$R_0 = \left[\frac{9(\ln 10)\Phi^D\kappa^2 J(\nu)}{128\pi^5 N_A n^4}\right]^{1/6},$$

where Φ^D is the quantum yield of the donor, $J(\nu)$ is the spectral overlap between the donor's emission and the acceptor's absorption, N_A is the Avogadro's number, n is the index of refraction of the medium, and κ^2 is determined by the relative orientation of the two dipole moments. We assumed $\kappa^2 = 2/3$ but this is only an approximation because the fluorescence anisotropy ranged from 0.2 to 0.3 for protein-conjugated Cy3 and was 0.3 for the Cy5 attached to DNA, indicating limited rotational motion within the radiative lifetime. All parameters except κ^2 were experimentally measured and used to calculate R_0 for each pair of fluorophores. In particular, Φ^D was measured for each Rep mutant singly labeled by Cy3 and ranged from 0.27 to 0.47, and corresponding R_0 against Cy5 at the partial duplex junction ranged from 61 Å to 65 Å.

Surface and sample cell preparations

To minimize non-specific adsorption of proteins and maximize specific binding of biotinylated DNA molecules, we prepared PEG surfaces that contain a small fraction (~1%) of biotinylated PEG molecules using the following procedure. First, the glass coverslips and quartz slides were soaked in a 1% (v/v) solution of an amino-silane reagent (Vectabond, Vector Labs.) in acetone and then soaked for three hours with a PEG solution, containing 25% (w/w) M-PEG-SPA M_r 5000 (Nektar Therapeutics) and 0.25% (w/w) biotin-PEG-SPA, M_r 3400 (Nektar Therapeutics) in 0.1 M sodium bicarbonate (pH 8.3). Once the surfaces were coated, we formed a sample cell by putting the PEG-coated side of the coverslip over the PEG-coated side of the quartz slide separated by a 100 μm thick spacer (3M double sided tape). Two 0.75 mm diameter holes were drilled into the quartz slide to form the inlet and outlet. Remaining boundaries between the sample cell and outside were sealed using epoxy. This technique has the advantage that many experimental conditions can be explored by flowing different solutions through the same sample cell. Small holes minimize evaporation during prolonged measurements and reduce oxygen uptake by the solution thereby reducing photobleaching effects. Once the sample cells are constructed they can

be kept in a dry environment for up to one week without degradation.

Single-molecule measurements

A wide-field total internal reflection fluorescence microscope based on an inverted microscope (IX70, Olympus) was used to image an area of 50 μm × 100 μm to an intensified CCD camera (iPentamax, Roper, operating at ten frames per second). Molecules were excited using a doubled Nd:YAG laser (532 nm, Crystalaser, power 10–20 mW at the sample plane) through a quartz prism placed over a quartz slide *via* a thin layer of immersion oil. The incident angle of the laser was controlled to achieve the total internal reflection at the interface between the quartz slide and aqueous imaging buffer. Fluorescently labeled DNA molecules are attached to this interface and the excitation intensity decays exponentially from the interface so that background fluorescence arising from the fluorophores in solution can be minimized. The laser light was linearly polarized for the data presented but signals were not dependent on the laser polarization, indicating relatively free rotation of the fluorophores in the laboratory frame. Fluorescence signal was collected using a water immersion objective (Olympus; 60 ×, 1.2 numerical aperture). After rejecting the scattered laser light using a long pass interference filter at 550 nm (Chroma), the imaging area was defined using a vertical slit (width 3 mm) located at the imaging plane of the microscope just outside the left side port. The emission is subsequently collimated using a 12 cm focal length achromat lens (Oriel), is split by a long pass extended reflection dichroic mirror at 635 nm (Chroma), is recombined using an identical dichroic mirror after reflecting off a mirror each, and is finally imaged onto the CCD using a 24 cm focal length achromat lens (Oriel) thereby achieving 2× magnification. Donor and acceptor images are laterally displaced by tilting the mirrors so that each image occupies one half of the camera. An independent calibration of the detection system using immobilized, fluorescent beads allows the construction of a mathematical mapping between the two imaging channels. Each fluorescent spot in the donor channel has a corresponding one in the acceptor channel, coming from the same spot in the sample. Ideally, one channel would map onto the other by a pure translation but aberrations introduced by the optical system make the mapping algorithm more complex. In a typical sample we can observe about 200 molecules in the imaging area. All single-molecule measurements were performed in buffer U with an oxygen scavenger system (0.1 mg/ml glucose oxidase, 0.02 mg/ml catalase, 1% β-mercaptoethanol and 0.4% (w/w) β-D-glucose) to increase the photo-stability of the fluorophores. All data were acquired using software written in Visual C++ (Microsoft) and analyzed using programs written in IDL (Research systems) to obtain time records of donor and acceptor fluorescence intensities of single molecules as a function of time.

Acknowledgements

We thank the National Institutes of Health (T.H. (GM65367) and T.M.L. (GM45948)) and the National Sciences Foundation (T.H.) for support of this work. We also thank Dr Katherine Brendza for performing single-turnover DNA unwinding experiments with some of the Rep mutants.

References

1. Cheng, W., Hsieh, J., Brendza, K. M. & Lohman, T. M. (2001). *E. coli* Rep oligomers are required to initiate DNA unwinding *in vitro*. *J. Mol. Biol.* **310**, 327–350.
2. Ha, T., Rasnik, I., Cheng, W., Babcock, H. P., Gauss, G., Lohman, T. M. & Chu, S. (2002). Initiation and reinitiation of DNA unwinding by the *Escherichia coli* Rep helicase. *Nature*, **419**, 638–641.
3. Lohman, T. M. & Bjornson, K. P. (1996). Mechanisms of helicase-catalyzed DNA unwinding. *Annu. Rev. Biochem.* **65**, 169–214.
4. Weiss, S. (1999). Fluorescence spectroscopy of single biomolecules. *Science*, **283**, 1676–1683.
5. Moerner, W. E. & Orrit, M. (1999). Illuminating single molecules in condensed matter. *Science*, **283**, 1670–1676.
6. Korolev, S., Hsieh, J., Gauss, G. H., Lohman, T. M. & Waksman, G. (1997). Major domain swiveling revealed by the crystal structures of complexes of *E. coli* Rep helicase bound to single-stranded DNA and ATP. *Cell*, **90**, 635–647.
7. Velankar, S. S., Soultanas, P., Dillingham, M. S., Subramanya, H. S. & Wigley, D. B. (1999). Crystal structures of complexes of PcrA DNA helicase with a DNA substrate indicate an inchworm mechanism. *Cell*, **97**, 75–84.
8. Subramanya, H. S., Bird, L. E., Brannigan, J. A. & Wigley, D. B. (1996). Crystal structure of a Dexx box DNA helicase. *Nature*, **384**, 379–383.
9. Maluf, N. K., Fischer, C. J. & Lohman, T. M. (2003). A dimer of *Escherichia coli* UvrD is the active form of the helicase *in vitro*. *J. Mol. Biol.* **325**, 913–935.
10. Dillingham, M. S., Wigley, D. B. & Webb, M. R. (2002). Direct measurement of single-stranded DNA translocation by PcrA helicase using the fluorescent base analogue 2-aminopurine. *Biochemistry*, **41**, 643–651.
11. Dillingham, M. S., Wigley, D. B. & Webb, M. R. (2000). Demonstration of unidirectional single-stranded DNA translocation by PcrA helicase: measurement of step size and translocation speed. *Biochemistry*, **39**, 205–212.
12. Jezewska, M. J., Rajendran, S., Bujalowska, D. & Bujalowski, W. (1998). Does single-stranded DNA pass through the inner channel of the protein hexamer in the complex with the *Escherichia coli* Dnab Helicase—fluorescence energy transfer studies. *J. Biol. Chem.* **273**, 10515–10529.
13. Scott, J. F., Eisenberg, S., Bertsch, L. L. & Kornberg, A. (1977). A mechanism of duplex DNA replication revealed by enzymatic studies of phage phi X174: catalytic strand separation in advance of replication. *Proc. Natl Acad. Sci. USA*, **74**, 193–197.
14. Ramirez-Carrozzi, V. & Kerppola, T. (2001). Gel-based fluorescence resonance energy transfer (gel-FRET) analysis of nucleoprotein complex architecture. *Methods*, **25**, 31–43.
15. Sofia, S. J., Premnath, V. & Merrill, E. W. (1998). Poly(ethylen oxide) grafted to silicon surfaces: grafting density and protein adsorption. *Macromolecules*, **31**, 5059.

16. Prime, K. L. & Whitesides, G. M. (1991). Self-assembled organic monolayers: model systems for studying adsorption of proteins at surfaces. *Science*, **252**, 1164.
17. Deniz, A. A., Dahan, M., Grunwell, J. R., Ha, T. J., Faulhaber, A. E., Chemla, D. S. *et al.* (1999). Single-pair fluorescence resonance energy transfer on freely diffusing molecules: observation of Forster distance dependence and subpopulations. *Proc. Natl Acad. Sci. USA*, **96**, 3670–3675.
18. Ha, T. J., Ting, A. Y., Liang, J., Caldwell, W. B., Deniz, A. A., Chemla, D. S. *et al.* (1999). Single-molecule fluorescence spectroscopy of enzyme conformational dynamics and cleavage mechanism. *Proc. Natl Acad. Sci. USA*, **96**, 893–898.
19. Mekler, V., Kortkhonjia, E., Mukhopadhyay, J., Knight, J., Revyakin, A. & Kapanidis, A. N. (2002). Structural organization of bacterial RNA polymerase holoenzyme and the RNA polymerase–promoter open complex. *Cell*, **108**, 599–614.
20. Schuler, B., Lipman, E. A. & Eaton, W. A. (2002). Probing the free-energy surface for protein folding with single- molecule fluorescence spectroscopy. *Nature*, **419**, 743–747.
21. Rothwell, P. J., Berger, S., Kensch, O., Felekyan, S., Antonik, M., Wohrl, B. M. *et al.* (2003). Multiparameter single-molecule fluorescence spectroscopy reveals heterogeneity of HIV-1 reverse transcriptase: primer/template complexes. *Proc. Natl Acad. Sci. USA*, **100**, 1655–1660.
22. Chao, K. & Lohman, T. M. (1991). DNA-induced dimerization of the *Escherichia coli* Rep helicase. *J. Mol. Biol.* **221**, 1165–1181.
23. Bjornson, K. P., Hsieh, J., Amaratunga, M. & Lohman, T. M. (1998). Kinetic mechanism for the sequential binding of two single-stranded oligodeoxynucleotides to the *Escherichia coli* Rep helicase dimer. *Biochemistry*, **37**, 891–899.
24. Chao, K. & Lohman, T. M. (1990). DNA and nucleotide-induced conformational changes in the *Escherichia coli* Rep and helicase II (UvrD) proteins. *J. Biol. Chem.* **265**, 1067–1076.
25. Cheng, W., Brendza, K. M., Gauss, G. H., Korolev, S., Waksman, G. & Lohman, T. M. (2002). The 2B domain of the *Escherichia coli* Rep protein is not required for DNA helicase activity. *Proc. Natl Acad. Sci. USA*, **99**, 16006–16011.
26. Colasant, J. & Denhardt, D. T. (1987). The *Escherichia coli* rep mutation. X. Consequences of increased and decreased Rep protein levels. *Mol. Gen. Genet.* **209**, 382–390.
27. Clegg, R. M. (1992). Fluorescence resonance energy transfer and nucleic acids. *Methods Enzymol.* **211**, 353–388.

Edited by D. E. Draper

(Received 30 September 2003; received in revised form 8 December 2003; accepted 10 December 2003)